Journal of Applied Physics ARTICLE scitation.org/journal/jap

Effects of InAlN underlayer on deep traps detected in near-UV InGaN/GaN single quantum well light-emitting diodes

Cite as: J. Appl. Phys. **126**, 125708 (2019); doi: 10.1063/1.5122314
Submitted: 1 August 2019 · Accepted: 3 September 2019 ·
Published Online: 26 September 2019

A. Y. Polyakov,[1] C. Haller,[2] N. B. Smirnov,[1] A. S. Shiko,[1] I. V. Shchemerov,[1] S. V. Chernykh,[1] L. A. Alexanyan,[1] P. B. Lagov,[1,3] Yu. S. Pavlov,[3] J.-F. Carlin,[2] M. Mosca,[2,4] R. Butté,[2] N. Grandjean,[2] and S. J. Pearton[5,a)]

AFFILIATIONS

[1]National University of Science and Technology MISiS, Moscow 119049, Russia
[2]Institute of Physics, Ecole Polytechnique Fédérale de Lausanne (EPFL), CH-1015 Lausanne, Switzerland
[3]Laboratory of Radiation Technologies, A. N. Frumkin Institute of Physical Chemistry and Electrochemistry Russian Academy of Sciences (IPCE RAS), Moscow 119071, Russia
[4]Department of Engineering, University of Palermo, I-90128, Palermo, Italy
[5]Department of Materials Science and Engineering, University of Florida, Gainesville, Florida 32611, USA

Note: This paper is part of the Special Topic on Defects in Semiconductors 2020.
[a)]**Author to whom correspondence should be addressed:** spear@mse.ufl.edu

ABSTRACT

Two types of near-UV light-emitting diodes (LEDs) with an InGaN/GaN single quantum well (QW) differing only in the presence or absence of an underlayer (UL) consisting of an InAlN/GaN superlattice (SL) were examined. The InAlN-based ULs were previously shown to dramatically improve internal quantum efficiency of near-UV LEDs, via a decrease in the density of deep traps responsible for nonradiative recombination in the QW region. The main differences between samples with and without UL were (a) a higher compensation of Mg acceptors in the *p*-GaN:Mg contact layer of the sample without UL, which correlates with the presence of traps with an activation energy of 0.06 eV in the QW region, (b) the presence of deep electron traps with levels 0.6 eV below the conduction band edge (E_c) (ET1) and at E_c 0.77 eV (ET2) in the *n*-GaN spacer underneath the QW, and the presence of hole traps (HT1) in the QW, 0.73 eV above the valence band edge in the sample without UL (no traps could be detected in the sample with UL), and (c) a high density of deep traps with optical ionization energy close to 1.5 eV for the LEDs without UL. Irradiation with 5 MeV electrons led to a strong decrease in the electroluminescence (EL) intensity in the LEDs without UL, while for the samples with UL, such irradiation had little effect on the EL signal at high driving current, although the level of driving currents necessary to have a measurable EL signal increased by about an order of magnitude. This is despite the 5 times higher starting EL signal of the sample with UL. Irradiation also led to the appearance in the LEDs with UL of the ET1 and HT1 deep traps, but with concentration much lower than without the UL, and to a considerable increase in the Mg compensation ratio.

I. INTRODUCTION

InGaN/GaN quantum well (QW) light-emitting diodes (LEDs) are efficient electroluminescence (EL) sources in the near-UV/blue spectral region, demonstrating peak internal quantum efficiency (IQE) > 85%.[1] These are currently used in general lighting systems, for backlighting of displays, in metrology, and in different indicator systems.[2] Hence, understanding how different growth conditions influence the performance of such devices is important. Growth of the InGaN/GaN QW region on top of InGaN or InAlN has a beneficial effect on LED efficiency.[3–9] Recent studies[7,8] suggest this is not related to differences in strain, dislocation density, or density of major contaminating impurities. It has been proposed[6–8] that the cause of the improvements in performance lies with the kinetics of formation and burying of surface defects in the In-containing sublayers. Without In-containing sublayers, these surface defects are believed to penetrate into the active QW region and form deep level

complexes, giving rise to strong nonradiative recombination.[6–8] Analysis of the efficiency of this process as a function of growth parameters—composition and thickness of the sublayer, growth temperature—suggested participation of nitrogen vacancy (V_N) related complexes with defects in the In sublattice to be the major suspects.[7,8] Based on recent results,[10] divacancies were suspected to be involved, and from the results of deep level optical spectroscopy (DLOS),[6] it was tentatively suggested that defects with optical ionization threshold near 1.6 eV are responsible.

In this paper, a thorough analysis using capacitance-voltage (*C-V*) profiling in the dark and under illumination, admittance spectroscopy (AS), and deep level transient spectroscopy (DLTS) measurements on pristine samples and samples subjected to electron irradiation sheds additional light on the nature of the observed processes.

II. EXPERIMENTAL

The LED structures investigated were similar to the InGaN/GaN single QW LED structures with and without InAlN/GaN superlattice (SL) underlayer (UL) described elsewhere.[9] Those were grown by metalorganic vapor phase epitaxy on GaN-on-sapphire templates in an Aixtron 200/4 RF-S horizontal reactor. The LED layer structure with InAlN SL UL is shown in Fig. 1. The growth started with a 2-μm-thick Si-doped GaN buffer followed by a 22-period $In_{0.17}Al_{0.83}N$:Si(2.1 nm)/GaN:Si(1.75 nm) SL with [Si] = 3×10^{18} cm^{-3}. Two more periods of the InAlN:Si/GaN:Si SL doped to 1.5×10^{20} cm^{-3} were grown on top and capped with a 5-nm-thick GaN layer with the same doping level and a 20-nm-thick GaN spacer doped with Si to $\sim3\times10^{18}$ cm^{-3}. This layer sequence was followed by the growth of a 2.7-nm-thick $In_{0.1}Ga_{0.9}N$ QW sandwiched between two 7.5 nm-thick *n*-GaN barriers ([Si] = 1×10^{18} cm^{-3}) that were subsequently capped with a 20-nm-thick undoped GaN spacer. The structure was completed with the growth of a 20-nm-thick *p*-$Al_{0.2}Ga_{0.8}N$:Mg electron blocking layer (EBL), a 200-nm-thick *p*-GaN:Mg layer ([Mg] $\approx1\times10^{19}$ cm^{-3}), and a 25-nm-thick *p*-GaN:Mg film doped to 1×10^{20} cm^{-3}, the role of the latter being to decrease the contact resistance with the *p*-contact layer. This sample is labeled InAlN UL LED.

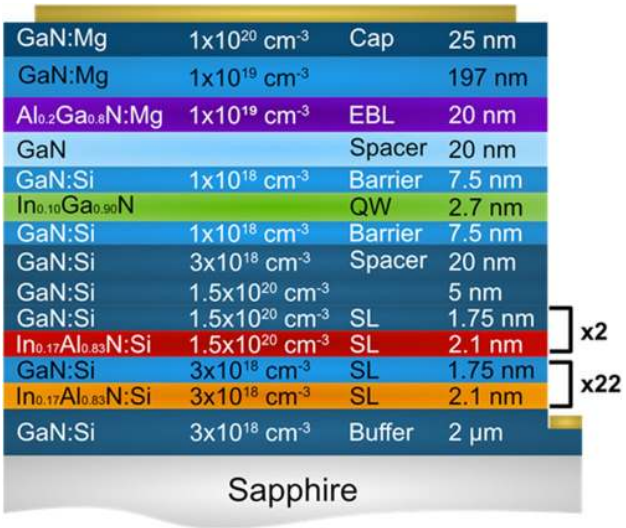

FIG. 1. Schematic representation of the layer sequence of the near-UV single QW LED with InAlN/GaN SL UL.

The sample without InAlN SL UL differed by the growth of the 5-nm-thick GaN spacer with the Si doping of 3×10^{18} cm^{-3} right after the 2-μm-thick Si-doped GaN buffer layer, i.e., the absence of the InAlN:Si/GaN:Si SL sequence. This latter sample, whose detailed description of the growth procedure can be found elsewhere,[9] is labeled NO UL LED.

The samples were processed into LEDs using conventional photolithography and dry etching. Ohmic contacts were fabricated by evaporating *p*-type Pd/Au and *n*-type Ti/Al/Ti/Au contact layers. All measurements were completed on 300×300 μm^2 chips contacted by wire bonding (Fig. 1S in the supplementary material shows an image of the LEDs).

Characterization included current-voltage (*I-V*), *C-V*, AS,[11] and DLTS[12] in the range of 77–400 K.[13–15] The relative intensities of the EL signal as a function of driving current were measured with 100 ms long forward current pulses with a 500 ms period and measuring the intensity from the current of a Si photodiode biased at +2 V with a Keysight Instruments current-voltage source meter B2902A was used.[16] Absolute measurements of the EL output power and IQE were not done in these experiments but were performed for LEDs before irradiation in an earlier work that showed the EL spectrum to be peaked near 3 eV for both samples and the IQE to ~70% for the InAlN UL LED and 9% for the NO UL LED.[9]

The measurements were repeated after irradiation at room temperature with 5 MeV electrons with a fluence of 7×10^{15} cm^{-2}, performed on the linear electron accelerator Linac UELV-10-10-C-70[17,18] at the Center of Collective Use "Physical Measurements Investigations" (CCU PMI) of the Institute of Physical Chemistry and Electrochemistry of the Russian Academy of Sciences.

III. RESULTS AND DISCUSSION

The RT *I-V* characteristics of the two structures in the dark and under 400 nm LED illumination creating electron-hole pairs in the single QWs are shown in Fig. 2(a). The reverse leakage current is considerably higher for the NO UL LED sample, and this leakage impacts the shape of the forward current for voltages <~1 V. For the InAlN UL LED, the reverse leakage current and the leakage in the forward voltage direction at low voltages are about two orders of magnitude lower. For forward voltages above ~1.5 V, the current grows exponentially with voltage with an ideality factor (η) of 2.3 and a saturation current density 6×10^{-22} A/cm^2. For both samples, the forward current shows almost a plateau for voltages above ~2 V and then grows exponentially with $\eta = 3.2$ and saturation current density $J_s = 4.5\times10^{-14}$ A/cm^2 (InAlN UL LED) or $\eta = 3.9$ and $J_s = 4.7\times10^{-13}$ A/cm^2 (NO UL LED) (in this latter case, the range of voltages corresponds to the onset of efficient double injection into the heterojunction). The series resistance of

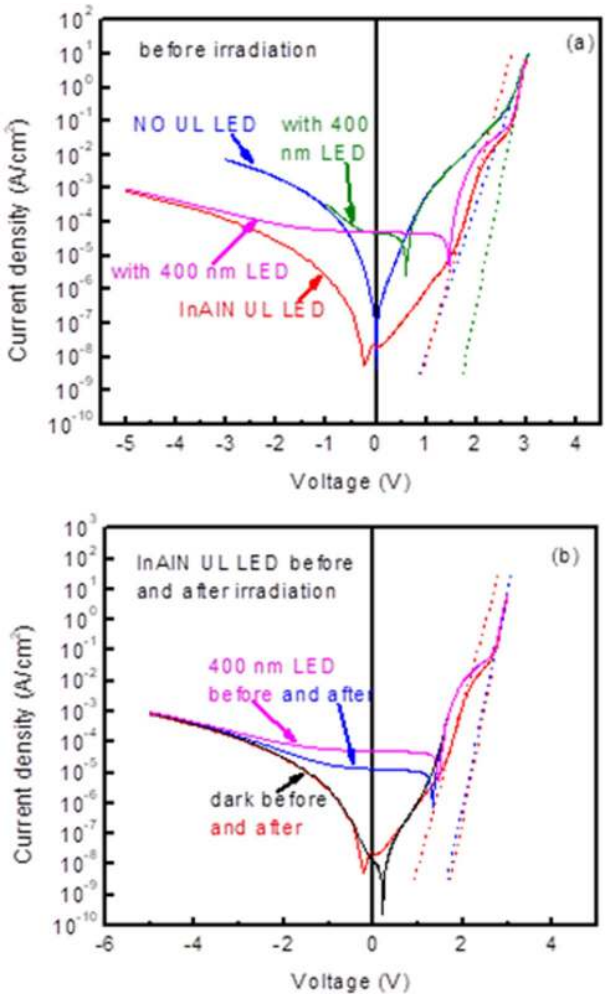

FIG. 2. (a) Room temperature current-voltage characteristics for the InAlN UL LED sample in the dark (red curve) and with 400 nm LED illumination (250 mW optical power, magenta curve) as compared to the respective characteristics for the NO UL LED sample (blue curve in the dark and olive curve under illumination). (b) Dark *I-V* characteristic before (black line) and after (red line) irradiation for the InAlN UL LED. The magenta line shows the photocurrent measured with the 400 nm LED excitation before irradiation, while the blue line shows the same photocurrent after irradiation.

the LED sample with InAlN UL is lower than that of the LED sample without UL (2 Ω vs 4.8 Ω). Finally, the short circuit current with 400 nm LED excitation is close for both structures; however, the open circuit voltage is higher for the sample with InAlN UL (1.46 V vs 0.6 V) as a consequence of stronger leakage.

Irradiation of the InAlN UL LED sample with 5 MeV electrons at a fluence of 7×10^{15} cm^{-2} leads to a slight increase in the series resistance (from 2 Ω to 3.3 Ω), a shift of the first step in the forward *I-V* characteristic from 1.6 V to 1.9 V, a decrease by a factor of about four in photocurrent density with 400 nm LED excitation (from 5.1×10^{-5} A/cm^2 to 1.4×10^{-5} A/cm^2) and a decrease in the open circuit voltage (from 1.46 V to 1.33 V) [Fig. 2(b)].

For the sample without InAlN UL, irradiation causes virtually no changes in the series resistance; however, it increases η from 3.9 to 4.1 and J_s from 4.7×10^{-13} A/cm^2 to 1.3×10^{-12} A/cm^2. The short circuit photocurrent decreases from 4.6×10^{-5} to 6.3×10^{-6} A/cm^2, and the open circuit voltage changes from 0.6 V before to 0.33 V after irradiation (the actual results can be viewed as Fig. 2S of the supplementary material). Thus, the changes induced by irradiation in the sample without InAlN UL are more profound than in the sample with UL, particularly, in terms of the generation-recombination in the QW region.

Figures 3(a) and 3(b) compare the density of charge centers as a function of depth and applied voltage for the two diodes (the data are obtained from *C-V* profiling). The profiles of the sample

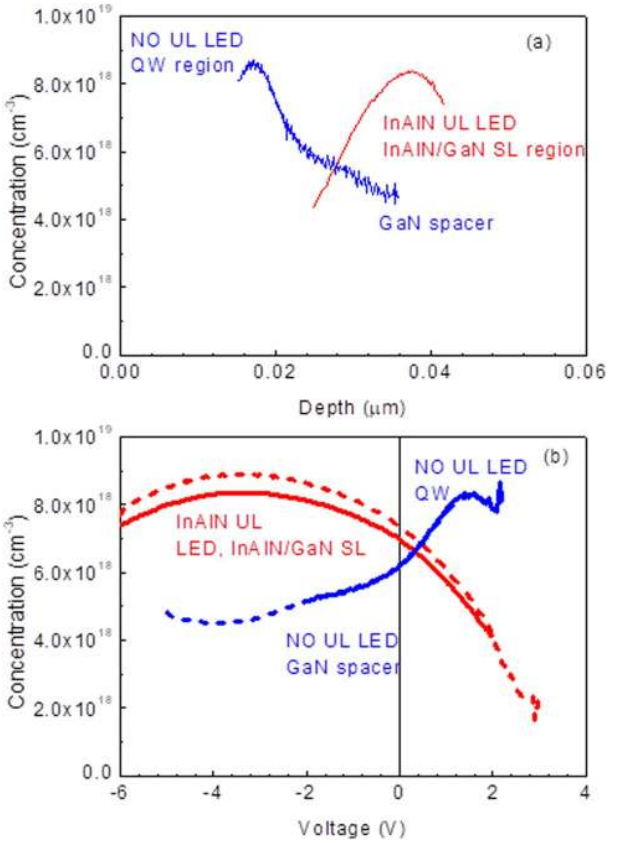

FIG. 3. (a) Charge concentration profiles in the space charge region determined from C-V measurements for the two LEDs. (b) Charge concentration vs applied voltage for the two studied LEDs before (solid lines) and after (dashed lines) irradiation with 5 MeV electrons at a fluence of 7×10^{15} cm^{-2}. The blue lines correspond to the NO UL LED, while the red lines correspond to the InAlN UL LED.

without UL clearly show the QW region and the GaN spacer region. The QW region could only be probed under forward bias. In DLTS, the traps located in the GaN spacer can be probed by biasing the sample at −3 V and pulsing the voltage to 0 V. The traps in the QW can be probed by keeping the sample at low reverse bias (e.g., −0.5 V) and pulsing to voltages above 2 V. At that stage, one cannot avoid injecting holes and the DLTS signal will be a mixture of electron trap and hole trap signals. Electron irradiation produces little effect on the trap concentration profile of the sample without InAlN UL, but slightly increases the apparent charge concentration in the InAlN/GaN SL and slightly shifts the entire *C-V* profile toward more negative voltages.

For the InAlN UL LED, the QW region needs the application of even higher forward voltages for *C-V* probing and could not be revealed even for forward biases of 2.5–3 V. The main feature in concentration vs depth and concentration vs voltage profiles is due to the GaN spacer/InAlN/GaN SL beneath the QW region. In DLTS, one is left with the only option of probing the traps in the QW region by keeping the quiescent bias at low values ∼−0.5 V and pulsing to +3 V which, according to the *I-V* characteristics in Fig. 2, definitely injects carriers into the QW region. For probing the GaN spacer/InAlN/GaN SL, the bias/pulse sequence of −5 V to −1 V will provide information on electron traps in this region.

With DLTS spectra measurements in GaN-based LEDs, one has to bear in mind that holes in the *p*-GaN cap are provided by Mg acceptors with an activation energy about 0.16 eV, and strongly freeze out at temperatures below ∼200 K. Hence, it leads to marked capacitance freeze out, preventing any meaningful DLTS measurements to be conducted at low temperatures.[16,17–22] For this reason, AS measurements were undertaken for studying the LEDs before and after electron irradiation. Figure 4(a) compares the temperature dependences of capacitances for frequencies *f* ranging from 0.3 kHz to 1 MHz for the two studied samples. Figure 4(b) compares the respective AC conductances *G* divided by the angular frequency $\omega = 2\pi f$, G/ω.[11] The measurements were performed at −0.2 V, placing the space charge region boundary close to the edge of the QW region for the sample with no InAlN UL and in the GaN spacer beneath the QW in the sample with InAlN UL.

The temperature at which capacitance starts to strongly freeze out is much higher for the sample without InAlN UL. This sample shows an additional low temperature capacitance freeze out region below ∼150 K, which is likely due to capacitance freeze out occurring in the QW region. This latter freeze out is not observed for the InAlN UL LED sample. Standard AS analysis of the shift of the capacitance steps and that of the conductance peaks as a function of temperature with increasing frequency,[11] such as shown in Figs. 4(a) and 4(b), gives the activation energy of the first capacitance freeze out step to be 0.165 eV for the NO UL LED sample vs 0.116 eV for the InAlN UL LED sample (Fig. 5). This is likely related to Mg freeze out.[16,19–22] To achieve the highest possible hole injection efficiency, one needs a high Mg concentration, likely to form a broad acceptor band.[23] Under these conditions, the activation energy is determined by the width of the band, the overall Mg concentration, and the compensation ratio of Mg, i.e., the depth of the Fermi level within the acceptor band.[23]

The Mg concentration is not impacted by the presence of an InAlN UL, as confirmed by secondary ion mass spectrometry (SIMS).[8] Therefore, both samples should have similar Mg concentration as their growth was performed under the same conditions. We conclude that in the NO UL LED sample, an additional compensation of Mg acceptors takes place, increasing the activation energy of Mg (and the series resistance in the *I-V* characteristics). The presence of an additional capacitance step in AS spectra at low temperatures taking place after the freeze out of Mg and occurring in the vicinity of the QW region hints at the reason for such increased compensation. The activation energy of the process, close to 0.06 eV, is similar to the ionization energy reported for nitrogen vacancies V_N in GaN.[23,24] Although such defects are not thermodynamically favored in *n*-type GaN films,[25] they could form under nonequilibrium growth conditions and be preserved in the *p*-AlGaN/*p*-GaN layers above the QW region. Defects related to V_N could be inherited from surface defects buried during the QW

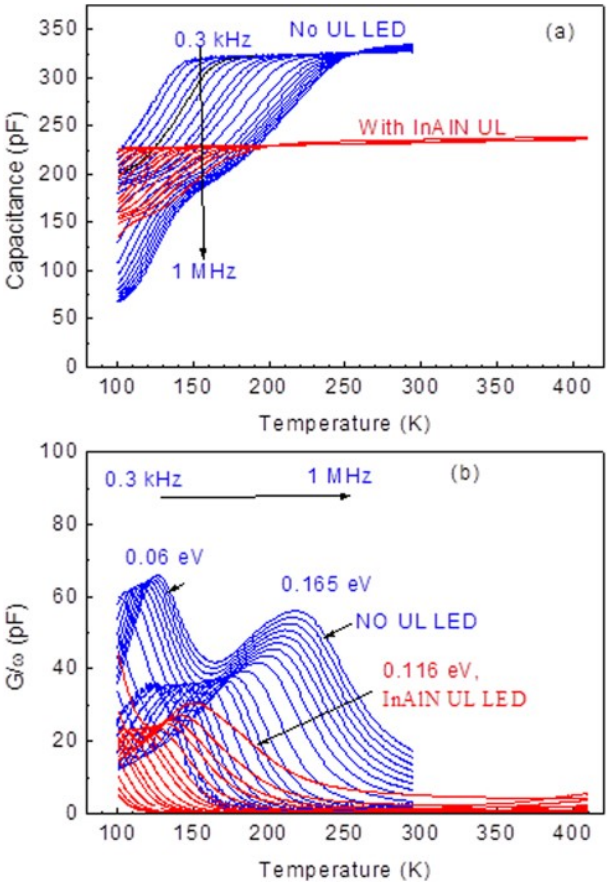

FIG. 4. (a) *C-f* dependences on temperature for frequencies ranging from 0.3 kHz (uppermost curves) to 1 MHz (lowermost curves) for the InAlN UL LED (red curves) and the NO UL LED (blue curves). (b) G/ω dependences on temperature for frequencies ranging from 0.3 kHz (leftmost curves) to 1 MHz (rightmost curves) for the InAlN UL LED (red curves) and the NO UL LED (blue curves).

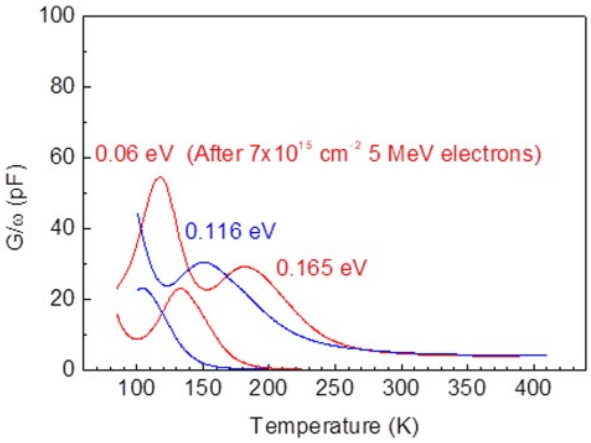

FIG. 5. Dependences of G/ω vs temperature for frequencies of 1 MHz (solid curves) and 10 kHz (dashed lines) for the InAlN UL LED before irradiation (blue curves) and after irradiation with 5 MeV electrons at a fluence of 7×10^{15} cm^{-2} (red curves). Note the emergence of the 0.06 eV center in the QW region and the increase in the activation energy related to the ionization of Mg acceptors from 0.116 eV to 0.165 eV after irradiation.

growth in the absence of any In-containing ULs and causing enhanced nonradiative recombination in the single QW region of such LEDs.[7–9] The lower Mg ionization energy deduced from the AS spectra of the InAlN UL LED and the absence of the 0.06 eV step in the AS spectra of this LED support such possibility. Moreover, irradiation causing the appearance of the 0.06 eV feature in these LEDs with InAlN UL neatly coincides with the increased activation energy of Mg acceptors (see Figs. 6 showing respective peaks in G/w for several frequencies, the temperature dependences of capacitances for the same frequencies can be viewed as Fig. 3S of the supplementary material).

AS measurements suggest that meaningful DLTS spectra could only be collected at temperatures above ~200 K. Figures 6(a) and 6(b) compare DLTS spectra taken for the LED sample without InAlN UL in the GaN spacer (biasing/pulsing voltages of −3 V/0 V) and in the QW region (biasing at −0.5 V and pulsing to 3 V). In the first spectra, there are two electron traps, ET1 and ET2, with levels located 0.6 eV below the conduction band edge (E_c) (electron capture cross section $\sigma_{n1} = 5.2 \times 10^{-16}$ cm^2) and at E_c 0.77 eV ($\sigma_{n2} = 2.3 \times 10^{-15}$ cm^2), respectively. These are the traps located in GaN and often observed in bulk GaN and in GaN LEDs.[16,19,21,23] The DLTS signal from the QW region is dominated by hole traps (HT1) with levels about 0.73 eV above the valence band edge (E_v), with a hole capture cross section σ_h of 2.3×10^{-15} cm^2, previously observed in some GaN-based LEDs.[21,26] Electron irradiation led to an increase in the density of deep traps in both the QW and the GaN spacer regions.[27]

In the sample with InAlN UL, no DLTS signal could be reliably detected either in the GaN spacer/InAlN/GaN SL (biasing at −5 V and pulsing to −1 V) or in the QW region (biasing at −0.5 V and pulsing to 3 V), indicating a much lower concentration of all traps. After irradiation, electron traps with a signature similar to

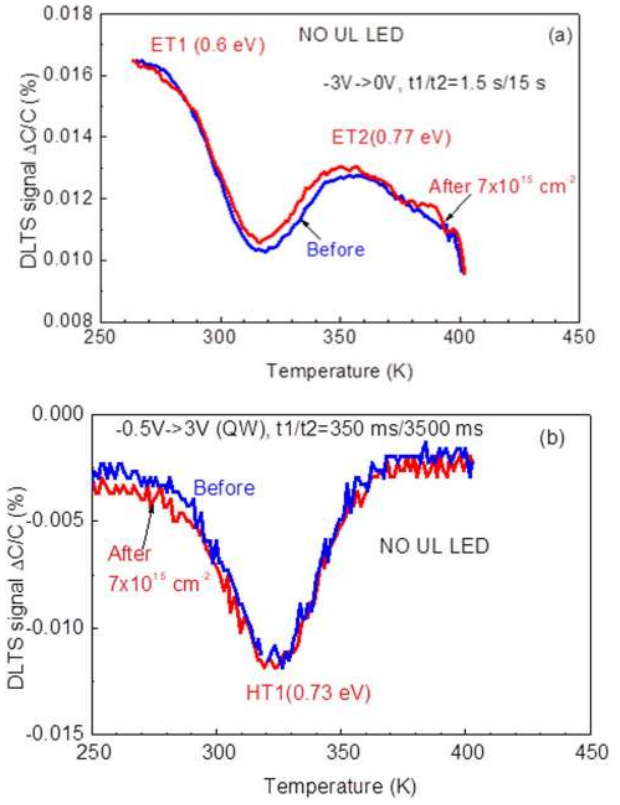

FIG. 6. (a) DLTS spectra measured with an applied voltage of −3 V and pulsing to 0 V (GaN spacer) for the NO UL LED sample before (blue line) and after (red line) irradiation with 5 MeV electrons at a fluence of 7×10^{15} cm^{-2}; (b) the spectra measured with the −0.5 V to 3 V bias/pulsing sequence probing the QW region; the time windows t1/t2 settings are shown in the figure.

the ET1 traps appear in the GaN spacer/InAlN/GaN SL region probed with biasing/pulsing sequence of −5 V to −1 V [Fig. 7(a)]. In the QW region, one observes deep hole traps similar to the HT1 $E_v + 0.73$ eV traps detected in the NO UL LED sample [Fig. 7(b)]. The magnitude of DLTS peaks after irradiation is still much lower than in the sample without InAlN UL, in agreement with the small changes in the concentrations of electron and hole traps observed in the latter sample subjected to electron irradiation. Emerging densities of traps in the LED sample with InAlN UL prior to any irradiation would allow one to reliably detect the growth of the density of the ET1 and HT1 traps after irradiation. Irradiation creates electron and hole traps similar to those that form following the incorporation of surface defects into the lattice during the growth of the LED sample without InAlN UL.

Figure 8 summarizes the Arrhenius signatures of the defects detected in AS and DLTS spectra, namely, the 0.06 eV centers in the QWs present both before and after irradiation in the LEDs without InAlN UL or introduced by irradiation in the InAlN UL LED, as well as the 0.116 eV Mg related feature in the InAlN UL

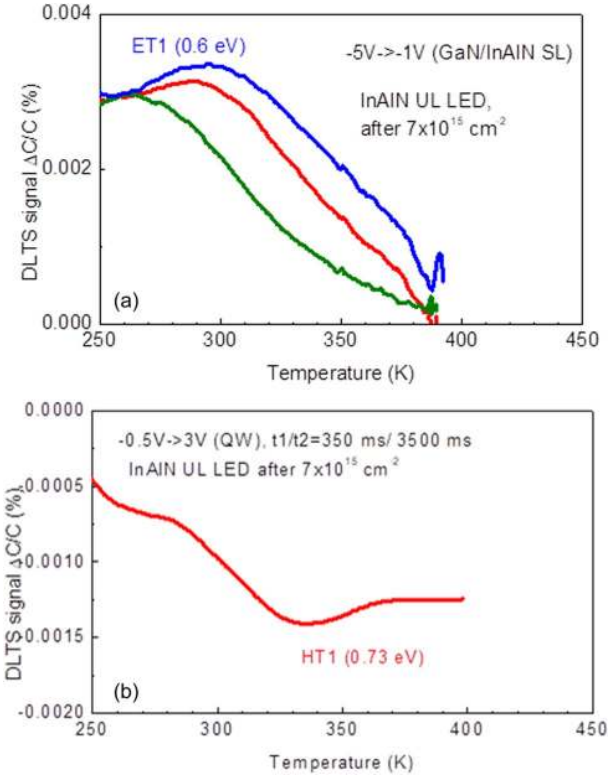

FIG. 7. (a) DLTS spectra measured on the InAlN UL LED sample after electron irradiation using a bias of −5 V and pulses of −1 V that allows probing the region of the GaN spacer/ InAlN/GaN SL. The data are shown for three t_1/t_2 time windows: 150 ms/1500 ms (blue curve), 350 ms/3500 ms (red curve), and 1750 ms/17 500 ms (olive curve). The ET1 electron trap signature can be clearly seen. (b) DLTS spectrum measured with pulsing from −0.5 V to 3 V (QW) using the time window t_1/t_2 = 350 ms/3500 ms.

LED and the 0.165 eV Mg feature in the NO UL LED or InAlN UL LED after irradiation. The ET1 electron traps and the HT1 hole traps, whose signatures are absent in the InAlN UL LED sample, but are present in the NO UL LED sample or do appear in the sample with InAlN UL after irradiation, are also shown. Traps found in the NO UL LED are identified via red symbols, while for the InAlN UL LED blue symbols are used. The ET2 electron traps are only observed in the NO UL LED samples both before and after electron irradiation and hence are only depicted by the red symbols.

The presence of InGaN underlayers is known to suppress the formation of deep traps with an optical ionization threshold energy close to 1.6 eV in single InGaN/GaN QWs.[6] The charge density in our NO UL LED QW is high so that the sensitivity is very limited. Furthermore, for the InAlN UL LED sample, we could probe the QW region by *C-V* profiling neither in the dark nor under illumination. However, for the NO UL LED sample, it was possible to measure the spectral changes in the *C-V* profiles under illumination

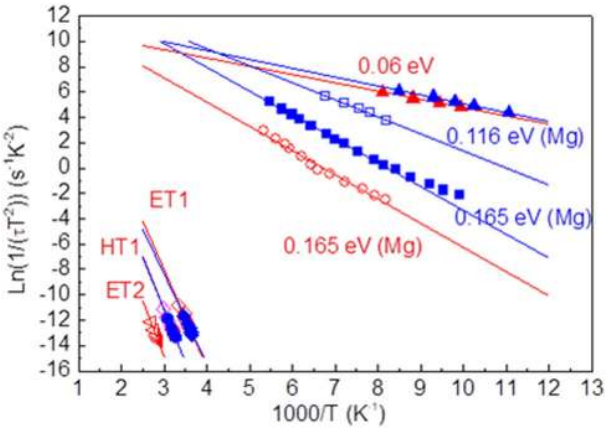

FIG. 8. Trap signatures for centers observed in admittance spectroscopy and DLTS; blue symbols refer to the sample without the InAlN underlayer, and red symbols refer to the sample with the InAlN underlayer.

before and after electron irradiation. The actual profiles obtained for several photon energies before irradiation are presented in Fig. 4S of the supplementary material. Such data for the sample before and after irradiation were used to build Fig. 9 that compares the spectral dependences of the concentrations deduced from *C-V* profiles obtained from excitation with different wavelengths for the NO UL LED sample before and after irradiation. These light *C-V* profiles show an optical threshold near a photon energy of 1.5 eV,[6] and the concentration is $\sim 4 \times 10^{16}$ cm^{-3} before irradiation and 9×10^{16} cm^{-3} after irradiation.

The comparison of the EL signal dependence on drive current before and after irradiation is shown in Fig. 10. Before irradiation,

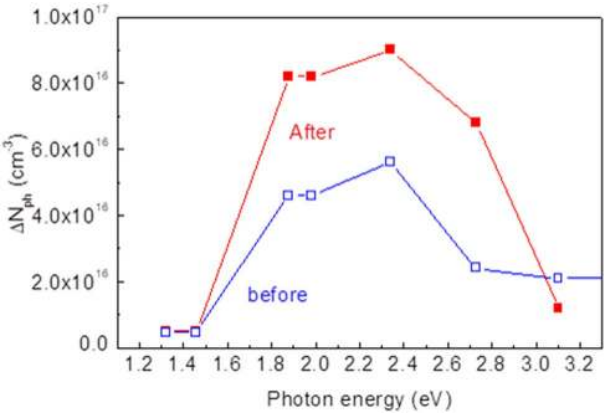

FIG. 9. Spectra of concentration changes, ΔN_{ph}, induced by illumination with photons of different energies for the QW region of the NO UL LED sample before (blue line) and after (red line) irradiation with 5 MeV electrons at a fluence of 7×10^{15} cm^{-2}.

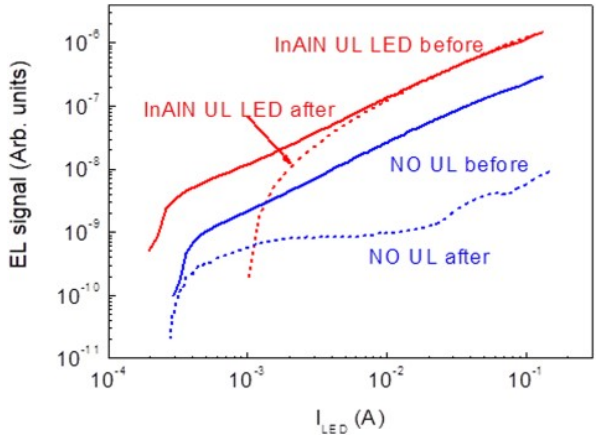

FIG. 10. EL intensity (in arbitrary units) as a function of the LED driving current for the InAlN UL LED (red lines) and the NO UL LED (blue lines) before (solid lines) and after (dashed lines) irradiation with 5 MeV electrons at a fluence of 7×10^{15} cm^{-2}.

the EL signal of the LED with InAlN UL is 5 times higher than without the UL. The electron irradiation introduces trap centers throughout the entire structure, but the most detrimental are the deep traps in the QW directly giving rise to nonradiative recombination and thus directly reducing efficiency, deep traps compensating p-type conductivity and increasing the series resistance, and deep traps in the QW barriers decreasing the injection efficiency. Deep traps in the InAlN UL are more benign in the sense that they only marginally affect the injection efficiency. Irradiation hardly changed the EL signal of the UL LED at high driving currents but increased the value of the driving current necessary to reliably detect the EL signal. By sharp contrast, for the LED without InAlN UL, exposure to high energy electrons led to a decrease in the EL signal throughout the range of injection currents, indicating that the density of recombination centers in the QW has increased. Given that the densities of deep traps in this LED are not strongly affected by electron irradiation, while the density of traps with the optical ionization threshold of 1.5 eV is substantially increased, one can speculate these centers are least, in part, responsible for the observed EL degradation.

The increase in the threshold driving current necessary to detect EL signals in the InAlN UL LED sample occurring after irradiation is most likely due to the increased compensation of Mg causing the increase in the series resistance and a decrease in the hole injection efficiency into the QW. Increased trapping by the ET1 and HT1 centers after irradiation could also contribute to this effect. If the EL efficiency in these LEDs is strongly impacted by the centers with an optical ionization threshold near 1.5 eV, as suspected for the LED sample without InAlN UL, one has to assume that the incorporation rate of these deep centers is seriously suppressed when growing an InAlN UL, otherwise the EL efficiency of InAlN UL LEDs should also be seriously altered. This is an important point that could have practical implications for improving the radiation tolerance of GaN-based LEDs.

IV. SUMMARY AND CONCLUSIONS

A major difference between near-UV single QW LED samples with and without InAlN/GaN SL UL is that the activation energy of Mg acceptor freeze out is higher without InAlN UL (0.165 eV vs 0.116 eV). The high concentration of Mg will form an impurity band for which the acceptor activation energy is determined by the concentration of Mg atoms and the position of the Fermi level within this impurity band. The higher the compensation ratio of Mg and hence the more filled the band, the higher the Fermi level and the measured activation energy. It is difficult to perform reliable Hall/Van der Pauw measurements directly on the grown LED structures with multilayer highly conducting region underlying the p-GaN:Mg region because of the parallel conduction. Since the Mg concentration is not impacted by the presence of an UL according to SIMS measurements[8] and knowing that the *p*-type region is grown under similar conditions for the two LEDs, one has to assume a stronger compensation of Mg takes place in the sample without UL. Surface defects incorporated into the single QW region, and that are responsible for enhanced nonradiative recombination, are very likely related to a nitrogen deficiency, i.e., defects of the nitrogen vacancy V_N type.[8] In the sample without InAlN UL, a prominent 0.06 eV trap, close to the level of V_N observed in electron irradiated *n*-GaN,[23,25] is present, which is not detected in the QW region with InAlN UL. This qualitatively fits the model proposed earlier.[7,8] A higher Mg compensation contributes to the higher series resistance without InAlN UL and could be responsible for the lower injection efficiency of holes and lower EL intensity. We also observe in the GaN spacer of the sample without InAlN UL, electron traps ET1 and ET2 with levels similar to the deep centers that adversely affect efficiency of blue and near-UV LEDs, via decreasing electron injection efficiency.[16,19–21] These traps, as well as HT1 hole traps present in the QW region, are absent in the LED sample with InAlN UL measured before irradiation, but the ET1 and HT1 traps appear in low concentration after electron irradiation. This suggests native defects form deep trap complexes similar to the ones formed by surface defects incorporated into the single QW region when no InAlN UL is used. These defects could play a role in decreasing the EL efficiency of the InAlN UL LEDs at low injection current observed after irradiation, although the increased compensation ratio of Mg after irradiation is of higher impact.

For the LED samples without InAlN UL, the role played by the ET1, ET2, and HT1 traps on EL degradation after bombardment with electrons is, however, not important for the low dose used here. The concentrations of the centers are not changed after irradiation whereas the EL intensity strongly decreases. The changes in the density of deep traps with optical ionization threshold near 1.5 eV following irradiation better fit the observed EL signal degradation. The incorporation rate in the QW region should be much lower than for LEDs without InAlN UL. Indeed, the data in Fig. 10 suggest that the density of the 1.5-eV-optical-threshold traps without InAlN UL almost doubles after irradiation. If the same incorporation rate were observed with InAlN UL and if the density of these traps indeed determined the EL efficiency, one would expect the EL signal of the sample with InAlN UL to be similar to the signal of LEDs without InAlN UL as a result of irradiation, which is not the case.

The use of an InAlN UL decreases the compensation ratio of Mg, improves injection efficiency in the active region, and decreases the series resistance. The density of electron and hole traps in the InAlN UL LED is lower than without InAlN UL. Electron irradiation likely introduces the same trap centers in the InAlN UL LEDs as those formed after incorporation of the surface defects in LEDs without UL. The radiation tolerance of LEDs with InAlN UL is higher than for similarly grown LEDs without UL, even though the EL efficiency of the former prior to irradiation is one order of magnitude larger.

SUPPLEMENTARY MATERIAL

The supplementary material shows images of the wire-bonded LED chips used for the characterization and additional current-voltage and capacitance-voltage characteristics from the irradiated devices. There are also some data on charge concentration profiles in the space charge region obtained from C-V measurements for the QW of the NO UL LED shown for several excitation photon energies.

ACKNOWLEDGMENTS

The work at EPFL was supported by the CTI-KTI project "High power GaN lasers for white light generation" No. 17519.1 PFEN-NM. The work of A. S. Shiko at NUST MISiS was supported in part by Grant No. K4-2018-024 under the Program to increase Competitiveness of NUST MISiS among the World Leading Scientific and Educational centers (program funded by the Russian Ministry of Science and Education). Electron irradiation was performed at the Center of Collective Use "Physical Measurements Investigations" (CCU PMI) of IPCE RAS.

REFERENCES

[1]A. David, N. G. Young, C. A. Hurni, and M. D. Craven, Appl. Phys. Lett. **110**, 253504 (2017).
[2]S. Nakamura, Angew. Chem. Int. Ed. **54**, 7770 (2015).
[3]S. F. Chichibu, A. Uedono, T. Onuma, B. A. Haskell, A. Chakraborty, T. Koyama, P. T. Fini, S. Keller, S. P. DenBaars, J. S. Speck, U. K. Mishra, S. Nakamura, S. Yamaguchi, S. Kamiyama, H. Amano, I. Akasaki, J. Han, and T. Sota, Nat. Mater. **5**, 810 (2006).
[4]T. Akasaka, H. Gotoh, T. Saito, and T. Makimoto, Appl. Phys. Lett. **85**, 3089 (2004).
[5]R. Butté, J.-F. Carlin, E. Feltin, M. Gonschorek, S. Nicolay, G. Christmann, D. Simeonov, A. Castiglia, J. Dorsaz, H. J. Buehlmann, S. Christopoulos, G. Baldassarri Höger von Högersthal, A. J. D. Grundy, M. Mosca, C. Pinquier, M. A. Py, F. Demangeot, J. Frandon, P. G. Lagoudakis, J. J. Baumberg, and N. Grandjean, J. Phys. D Appl. Phys. **40**, 6328 (2007).
[6]A. M. Armstrong, B. N. Bryant, M. H. Crawford, D. D. Koleske, S. R. Lee, and J. J. Wierer, J. Appl. Phys. **117**, 134501 (2015).
[7]C. Haller, J.-F. Carlin, G. Jacopin, D. Martin, R. Butté, and N. Grandjean, Appl. Phys. Lett. **111**, 262101 (2017).
[8]C. Haller, J.-F. Carlin, G. Jacopin, W. Liu, D. Martin, R. Butté, and N. Grandjean, Appl. Phys. Lett. **113**, 111106 (2018).
[9]C. Haller, J.-F. Carlin, M. Mosca, M. D. Rossell, R. Erni, and N. Grandjean, Appl. Phys. Express **12**, 034002 (2019).
[10]S. F. Chichibu, A. Uedono, K. Kojima, H. Ikeda, K. Fujito, S. Takashima, M. Edo, K. Ueno, and S. Ishibashi, J. Appl. Phys. **123**, 161413 (2018).
[11]J.-L. Pautrat, B. Katircioglu, N. Magnea, D. Bensahel, J.-C. Pfister, and L. Revoil, Solid-State Electron. **23**, 1159 (1980).
[12]D. K. Schroder, *Semiconductor Materials and Device Characterization* (John Wiley and Sons, New York, 1990), Chap. 7.
[13]A. Y. Polyakov, N. B. Smirnov, I.-H. Lee, and S. J. Pearton, J. Vac. Sci. Technol. B **33**, 061203 (2015).
[14]I.-H. Lee, A. Y. Polyakov, N. B. Smirnov, E. B. Yakimov, S. A. Tarelkin, A. V. Turutin, I. V. Shemerov, and S. J. Pearton, J. Appl. Phys. **119**, 205109 (2016).
[15]A. Y. Polyakov, N. B. Smirnov, E. B. Yakimov, I.-H. Lee, and S. J. Pearton, J. Appl. Phys. **119**, 015103 (2016).
[16]I.-H. Lee, A. Y. Polyakov, N. B. Smirnov, I. V. Shchemerov, P. B. Lagov, R. A. Zinov'ev, E. B. Yakimov, K. D. Shcherbachev, and S. J. Pearton, J. Appl. Phys. **122**, 115704 (2017).
[17]Y. S. Pavlov, A. M. Surma, P. B. Lagov, Y. L. Fomenko, and E. M. Geifman, J. Phys. Conf. Ser. **747**, 012085 (2016).
[18]Y. S. Pavlov and P. B. Lagov, in *2015 15th European Conference on Radiation and Its Effects on Components and Systems (RADECS)* (IEEE, 2015).
[19]A. Y. Polyakov, N. B. Smirnov, E. B. Yakimov, H.-S. Cho, J. H. Baek, A. V. Turutin, I. V. Shemerov, E. S. Kondratyev, and I.-H. Lee, ECS Solid State Sci. Technol. **5**, Q274 (2016).
[20]I.-H. Lee, A. Y. Polyakov, N. B. Smirnov, I. V. Shchemerov, N. M. Shmidt, N. A. Talnishnih, E. I. Shabunina, H.-S. Cho, S.-M. Hwang, R. A. Zinovyev, S. I. Didenko, P. B. Lagov, and S. J. Pearton, Phys. Status Solidi A **214**, 1700372 (2017).
[21]A. Y. Polyakov, N. B. Smirnov, I. V. Shchemerov, E. B. Yakimov, E. E. Yakimov, K. C. Kim, and I.-H. Lee, ECS Solid State Sci. Technol. **7**, Q80 (2018).
[22]A. Y. Polyakov, N. M. Shmidt, N. B. Smirnov, I. V. Shchemerov, E. I. Shabunina, N. A. Tal'nishnih, I.-H. Lee, L. A. Alexanyan, S. A. Tarelkin, and S. J. Pearton, J. Appl. Phys. **125**, 215701 (2019).
[23]A. Y. Polyakov and I.-H. Lee, Mater. Sci. Eng. R **94**, 1 (2015).
[24]S. J. Pearton, F. Ren, E. Patrick, M. E. Law, and A. Y. Polyakov, ECS Solid State Sci. Technol. **5**, Q35 (2016).
[25]C. G. Van de Walle and J. Neugebauer, J. Appl. Phys. **95**, 3851 (2004).
[26]I.-H. Lee, A. Y. Polyakov, N. B. Smirnov, R. A. Zinovyev, K.-B. Bae, T.-H. Chung, S.-M. Hwang, J. H. Baek, and S. J. Pearton, Appl. Phys. Lett. **110**, 192107 (2017).
[27]I.-H. Lee, A. Y. Polyakov, N. B. Smirnov, I. V. Shchemerov, T.-H. Chung, P. B. Lagov, R. A. Zinov'ev, and S. J. Pearton, ECS Solid State Sci. Technol. **6**, Q127 (2017).